THE JOURNAL OF PHYSICAL CHEMISTRY A

Article

pubs.acs.org/JPCA

Dissociative Photoionization of the Elusive Vinoxy Radical

Jonathan D. Adams,[†] Preston G. Scrape,[†] Shih-Huang Lee,[‡] and Laurie J. Butler*,[†]

[‡]National Synchrotron Radiation Research Center, Hsinchu 30076, Taiwan, Republic of China

[†]The James Franck Institute and Department of Chemistry, The University of Chicago, Chicago, Illinois 60637, United States

Supporting Information

ABSTRACT: These experiments report the dissociative photoionization of vinoxy radicals to m/z = 15 and 29. In a crossed laser−molecular beam scattering apparatus, we induce C−Cl bond fission in 2-chloroacetaldehyde by photoexcitation at 157 nm. Our velocity measurements, combined with conservation of angular momentum, show that 21% of the C−Cl photofission events form vinoxy radicals that are stable to subsequent dissociation to CH_3 + CO or H + ketene. Photoionization of these stable vinoxy radicals, identified by their velocities, which are momentum-matched with the higher-kinetic-energy Cl atom photofragments, shows that the vinoxy radicals dissociatively photoionize to give signal at m/z = 15 and 29. We calibrated the partial photoionization cross section of vinoxy to CH_3^+ relative to the bandwidth-averaged photoionization cross section of the Cl atom at 13.68 eV to put the partial photoionization cross sections on an absolute scale. The resulting bandwidth-averaged partial cross sections are 0.63 and 1.3 Mb at 10.5 and 11.44 eV, respectively. These values are consistent with the upper limit to the cross section estimated from a study by Savee et al. on the $O(^3P)$ + propene bimolecular reaction. We note that the uncertainty in these values is primarily dependent on the signal attributed to C−Cl primary photofission in the m/z = 35 (Cl^+) time-of-flight data. While the value is a rough estimate, the bandwidth-averaged partial photoionization cross section of vinoxy to HCO^+ calculated from the signal at m/z = 29 at 11.53 eV is approximately half that of vinoxy to CH_3^+. We also present critical points on the potential energy surface of the vinoxy cation calculated at the G4//B3LYP/6-311++G(3df,2p) level of theory to support the observation of dissociative ionization of vinoxy to both CH_3^+ and HCO^+.

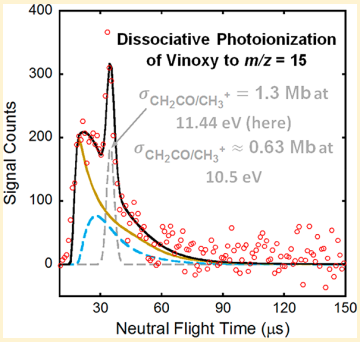

1. INTRODUCTION

Tunable single-photon ionization is a common method for detecting polyatomic products of unimolecular and bimolecular reactions because it is less likely to induce dissociative ionization compared to electron bombardment ionization.[1−3] While the photoionization cross sections of many stable polyatomic molecules have been determined,[4] it is often difficult to measure the photoionization cross sections of radicals and of excited-state species. To extract product branching fractions from ion intensity data when detecting products with photoionization, it is important to determine the total or partial photoionization cross section of the product of interest. One particular radical with interesting, but vexing, photoionization behavior is the vinoxy radical (CH_2CHO), an important intermediate in combustion.[5−9] While the adiabatic photoionization threshold of vinoxy is 9.3 eV,[10] the vertical photoionization threshold is 10.3 eV.[10,11] As such, it is difficult to detect vinoxy cation at its parent mass; indeed, the only experiment using photoionization detection to succeed in detecting vinoxy at m/z = 43 is that by Scrape et al.,[12] and the signal at the parent mass is quite small. Previous studies have shown that vinoxy undergoes dissociative photoionization to CH_3^+ + CO,[10,11] CH_2CO^+ + H,[10] and HCO^+ + CH_2,[12] but no absolute partial photoionization cross sections were determined. Of these dissociative ionization pathways, only the CH_3^+ + CO channel is significant at ionization energies close to the vertical photoionization threshold. The previous study by Savee et al.[11] detected the onset of dissociative ionization of vinoxy radical to CH_3^+ at 10.2 eV, but they were unable to determine a partial photoionization cross section due to contributions to the signal from the dissociative ionization of other species.

In this study, we photolytically produce vinoxy radicals by photodissociating 2-chloroacetaldehyde at 157 nm. Some of the nascent vinoxy radicals are stable to subsequent dissociation to CH_3 + CO or to H + ketene and, upon photoionization, undergo dissociative ionization to CH_3^+ and HCO^+. We detect the products from the dissociative ionization of the nascent vinoxy radicals, which are momentum-matched with the higher-kinetic-energy Cl cofragments. From the data, we estimate the relative partial photoionization cross sections of vinoxy to CH_3^+ at 10.5 and 11.44 eV. Using literature values[13,14] for the photoionization cross section of Cl atoms at 13.68 eV and averaging over the bandwidth of the photoionization source allows us to calculate the absolute partial photoionization cross section of vinoxy to CH_3^+. Because we determine the recoil kinetic energy of the photofragments from the time-of-flight (TOF) data, we can characterize the internal energy of the

Received: May 16, 2017
Revised: July 27, 2017
Published: August 14, 2017

DOI: 10.1021/acs.jpca.7b04730
J. Phys. Chem. A 2017, 121, 6262−6268

nascent vinoxy radicals. It is important to characterize the internal energy of the radical because the photoionization efficiency can depend on the internal energy[15] and electronic state[16] of the radical being ionized. Using our branching calculations (described in further detail in ref 17), we predict what portion of the nascent vinoxy radicals are stable to unimolecular dissociation and can thus undergo dissociative ionization. While vibrationally hot vinoxy can undergo unimolecular dissociation to CH_3 + CO, thus providing another source of signal at m/z = 15 (CH_3^+), the arrival times of the neutral CH_3 products and CH_3^+ from dissociative ionization are distinct in this scattering experiment, making these contributions easy to distinguish from one another.

2. EXPERIMENT

A detailed description of the experimental apparatus appears elsewhere;[18−20] we provide a brief description here. The data were taken at the National Synchrotron Radiation Research Center (NSRRC), in Hsinchu, Taiwan, using the U9 Chemical Dynamics Beamline and a crossed laser−molecular beam scattering apparatus. A 3% molecular beam of chloroacetaldehyde was created by first seeding the vapor pressure at 25 °C of the liquid sample (50% solution in water from Sigma-Aldrich, used without further purification) in neon with a total backing pressure of ∼600 Torr. The gaseous mixture was then supersonically expanded into a rotating source chamber through a pulsed nozzle with a 0.25 mm orifice. The nozzle operated at 100 Hz and was held at a temperature of 60 °C. The rotating source was set at an angle of 10 or 20° with respect to the detection axis. The molecular beam intersected the 157 nm unpolarized output of a LPF 200 Lambda Physik Laser Technik excimer laser propagating perpendicularly to the plane created by the molecular beam and the detection axis. The laser beam was focused to an area of ∼2.5 × 8 mm^2 at its intersection with the molecular beam, and the pulse energy was maintained at around 8 mJ.

Following photodissociation, the resulting fragments recoil with a range of net velocities representing the vector sum of the recoil velocities (from both primary C−Cl photofission and secondary dissociation of a portion of the vinoxy products formed with high internal energy) and the velocity of the precursor in the molecular beam. Those fragments with a net velocity vector pointing into the detector traveled 10.05 cm to enter the ionizer region, where they were ionized by tunable VUV synchrotron radiation. Photoionization energies were chosen by tuning the U9 undulator gap, and the input undulator radiation was defined by a 7 mm diameter circular aperture. The bandwidth of the synchrotron radiation was 4.2% full width at half-maximum, corresponding to 0.44 eV when the photoionization source was tuned to 10.5 eV. Higher harmonics of the VUV radiation were filtered out using a 30 cm gas cell containing ∼10 Torr of argon. The filtered undulator radiation was focused into an area of diameter ∼ 1 mm in the ionizer. The ionized fragments were then accelerated by a series of ion lenses through a quadrupole mass filter and counted by a Daly detector. The data reported herein were taken with a lower mass resolution than those in our previous studies at the NSRRC, so evidencing, for example, a contribution at m/z = 35 from signal a mass unit higher. These contributions were identified by their velocity distributions. A multichannel scaler recorded the signal count as a function of total TOF, which is the sum of the flight time of the neutral fragments to the ionizer and the flight time of the ionized fragments through the detector. The neutral flight time was recovered from the total TOF by subtracting the ion flight time calculated using the calibrated ion flight time coefficient of 5.43 μs $amu^{-1/2}$. Thus, we can easily recover the velocity of the neutral vinoxy radicals even when they are detected at a daughter fragment formed from the photoionization. The data were collected in 1 μs bins, and the TOF was corrected to account for the measured 1.1 μs electronic delay between the laser and the triggering of the multichannel scaler. All TOF spectra in the figures herein show the neutral flight time.

The TOF spectra were fit to recoil kinetic energy distributions ($P(E_T)$'s) by forward convolution fitting using the CMLAB2 program.[21] The molecular beam velocity was characterized using a photodepletion (hole-burning) technique. By operating the photolysis laser at 50 Hz and the pulsed nozzle at 100 Hz, only half of all molecular beam pulses underwent photodissociation. These measurements were taken with the rotating source chamber set on-axis with the detector. Subtracting the laser-off signal from the laser-on signal produced a hole-burned TOF spectrum, from which we determined the velocity distribution of the molecules in the molecular beam that undergo photodissociation. The velocity distribution typically had a maximal probability at 800 m/s and a full width at half-maximum of 270 m/s.

3. RESULTS

The data in Figure 1 measure the signal from the Cl photofragments produced from the photodissociation of 2-chloroacetaldehyde at 157 nm. Although we did not detect any of the vinoxy cofragment at the parent mass-to-charge ratio, we did observe CH_3^+ and HCO^+ fragments produced from the dissociative ionization of the stable vinoxy radicals. On the basis of our branching calculations (described below), about 21% of the C−Cl bond fission events produce vinoxy radicals that are stable to subsequent unimolecular dissociation. The dissociative ionization products have the distribution of arrival times predicted for stable vinoxy radicals as they are momentum-matched to the high-kinetic-energy Cl photofragments. As the

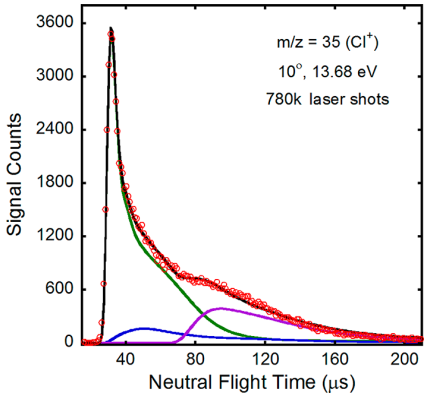

Figure 1. TOF spectrum taken at m/z = 35 (Cl^+) with a source angle of 10° and at an ionization energy of 13.68 eV. Data are shown in red circles. Primary C−Cl bond fission is fit by the solid green line using the $P(E_T)$ shown in Figure 2. The contribution from "bleed in" of m/z = 36 ($H^{35}Cl^+$) is shown with a solid blue line and is fit using the primary HCl photoelimination $P(E_T)$ in ref 22. The fit shown as the solid purple line represents the contribution attributed to photodissociation of clusters in the molecular beam.

DOI: 10.1021/acs.jpca.7b04730
J. Phys. Chem. A 2017, 121, 6262−6268

stable vinoxy radicals are produced in a 1:1 ratio with their momentum-matched Cl atoms, this allows us to determine the ratio between the partial photoionization cross section of vinoxy to CH_3^+ and the photoionization cross section of Cl at 13.68 eV. Because the m/z = 15 (CH_3^+) TOF data was taken at photoionization energies of 10.5 and 11.44 eV, we estimate the partial photoionization cross section at both of these energies. While the value is much rougher, we also estimate the partial photoionization cross section of vinoxy to HCO^+ at 11.54 eV.

Figure 1 shows the TOF spectrum taken at m/z = 35 (Cl^+) taken at a source angle of 10° and a photoionization energy of 13.68 eV. The experimental data are shown with open red circles. The distribution of recoil kinetic energies imparted in the dissociation, $P(E_T)$, is determined by forward convolution fitting of the contribution in the m/z = 35 (Cl^+) TOF spectra that is from primary C−Cl bond fission. The C−Cl bond fission $P(E_T)$ is shown with the green line in Figure 2, and its

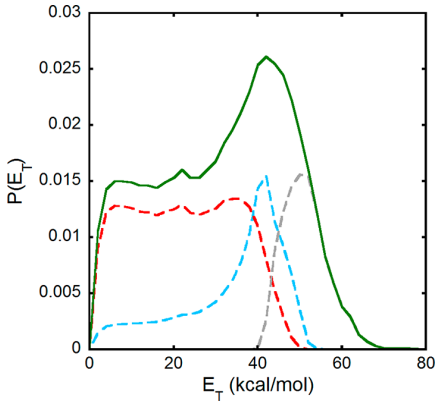

Figure 2. Photofragment recoil kinetic energy distribution for C−Cl bond fission in chloroacetaldehyde at 157 nm derived by forward convolution fitting of the signal at m/z = 35 (Cl^+). Results of the branching calculations using a barrier height of 44.6 kcal/mol for the H loss channel are also shown. The total primary C−Cl bond fission $P(E_T)$ derived from the scattering data is shown with a solid green line along with the predicted portions that produce H + ketene products (dashed red curve), methyl + CO products (dashed blue curve), and stable vinoxy radicals that do not dissociate (dashed gray curve). The "stable" portion of the $P(E_T)$ is the distribution of C−Cl photofission events that our model predicts partitions insufficient vibrational energy to surmount the isomerization barrier that neutral vinoxy radicals must pass to dissociate to CH_3 + CO.

corresponding fit to the TOF data is shown with the green line in Figure 1. The fit shown by solid blue line corresponds to "bleed in" from the m/z = 36 ($H^{35}Cl^+$) signal, which resulted from the low resolution of the quadrupole mass filter. Further information regarding these fits can be found in ref 22.

Because only stable vinoxy radicals will undergo dissociative photoionization, we used a rotational model to account for the partitioning of energy between rotation and vibration in the radical, allowing us to determine the portion of the C−Cl bond fission $P(E_T)$ that produces stable vinoxy fragments. Briefly, the model uses the measured recoil kinetic energies and angular momentum conservation to predict the portion of the C−Cl bond fission $P(E_T)$ that produces vinoxy radicals that are stable to subsequent dissociation by virtue of having vibrational energy below the lowest dissociation barrier. It also predicts the branching ratio between the H + ketene and CH_3 + CO product channels at each E_T. The model uses RRKM rate constants at the correct sums and densities of vibrational states while accounting for angular momentum conservation.[22] The portion of the primary C−Cl bond fission $P(E_T)$ producing stable vinoxy radicals is then obtained by subtracting the portion producing dissociative vinoxy radicals from the total $P(E_T)$. The results of the branching calculation are shown in Figure 2. The portion predicted to produce vinoxy radicals that dissociate to H + ketene is shown by the dashed red line, and the portion producing vinoxy radicals that dissociate to CH_3 + CO is shown by the dashed blue line. The dashed gray line depicts the portion of the C−Cl photofission $P(E_T)$ that produces high-kinetic-energy Cl atoms momentum-matched to vinoxy radicals that are stable to unimolecular dissociation; we used this "stable portion" to fit the signal from dissociative ionization of vinoxy to CH_3^+ in the m/z = 15 (CH_3^+) TOF data and to identify the signal from the momentum-matched Cl cofragments.

Figure 3 depicts the TOF spectra taken at m/z = 15 (CH_3^+) with a source angle of 10° and at ionization energies of 10.5 eV (top frame) and 11.44 eV (bottom frame). The sharp peak at

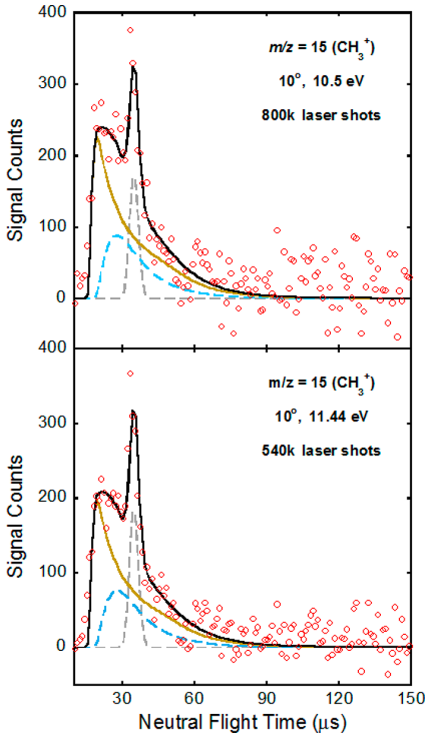

Figure 3. TOF spectra taken at m/z = 15 (CH_3^+) with a source angle of 10° and two different ionization energies. The upper frame shows the data taken at an ionization energy of 10.5 eV, and the lower frame shows the data taken at an ionization energy of 11.44 eV. Data are shown with red circles. The dashed blue fit shows the contribution from the dissociation of vibrationally hot vinoxy to CH_3 + CO and is calculated using the $P(E_T)$ shown with a dashed blue line in Figure 2 and accounting for the recoil of CH_3 from CO using the $P(E_T,2°)$ shown in ref 22 and an isotropic angular distribution. Dissociative ionization of stable vinoxy radicals to CH_3^+ is shown with a dashed gray line and was fit using the dashed gray line portion of the $P(E_T)$ in Figure 2. The olive-colored fit shows the contribution from the dissociation of vinoxy induced by absorption of another 157 nm photon.

DOI: 10.1021/acs.jpca.7b04730
J. Phys. Chem. A 2017, 121, 6262−6268

~34 μs is clearly distinguishable from the rest of the signal and scales differently with the photoionization energy used for detection than the rest of the signal. This peak is thus easily assigned to the dissociative photoionization of stable vinoxy radicals to CH_3^+ in the ionizer and thus has the same arrival times as the stable vinoxy radicals after accounting for the differing ion flight time. The fit for this contribution in the m/z = 15 TOF spectra is shown by the dashed gray line and was derived from the portion of the C−Cl bond fission $P(E_T)$ producing stable vinoxy radicals (shown by the dashed gray line in Figure 2). This fit is consistent with the arrival times of the sharp peak in the TOF spectra. The other contributions in the m/z = 15 (CH_3^+) TOF spectra are from secondary dissociation of the vibrationally excited vinoxy to CH_3 + CO and multiphoton dissociation of vinoxy to CH_3 + CO. The fits for these contributions are shown by the dashed blue line and solid olive-colored line, respectively. Further details regarding these fits can be found in ref 22. For the purposes of this paper, it is only worth noting that we can obtain a good fit to the rest of the signal in the TOF spectra and, more importantly, get a good fit to the slow side of the peak at 22 μs. Because the signal attributed to dissociative ionization is distinguishable from the rest of the signal and we can account for underlying signal from the peak at 22 μs, we can get a decent estimate of the amount of signal from dissociative ionization of vinoxy to CH_3^+ and thus determine the partial photoionization cross section of vinoxy to CH_3^+ by integrating under the fit for that contribution.

Because the quantum yield, ϕ, of stable vinoxy radicals and their momentum-matched Cl fragments from C−Cl bond fission is 1:1 and the photoionization cross section of Cl is known, the partial photoionization cross section for vinoxy appearing at CH_3^+, σ_{CH_2CHO/CH_3^+}, is given by

$$\frac{\phi_{Cl}}{\phi_{CH_2CHO}} = \frac{1}{1} = \text{obs}\left(\frac{^{35}Cl^+}{CH_3^+}\right) \times f_{^{35}Cl}{}^{-1} \times \text{TS}\left(\frac{CH_2CHO}{^{35}Cl}\right) \times \left(\frac{q_X}{q_{13.68\,eV}}\right) \times \left(\frac{\sigma_{CH_2CHO/CH_3^+}}{\sigma_{Cl/Cl^+}@13.68\ eV}\right) \quad (1)$$

where $\text{obs}\left(\frac{^{35}Cl^+}{CH_3^+}\right)$ is the observed signal from stable vinoxy in the m/z = 15 (CH_3^+) and m/z = 35 (Cl^+) data corrected for the number of laser shots, $f_{^{35}Cl}$ is the isotopic abundance of ^{35}Cl, $\text{TS}\left(\frac{CH_2CHO}{^{35}Cl}\right)$ is the correction for kinematic factors and the flight time through the ionization region, q_X is the photon flux at the photoionization energy used to collect the TOF spectrum (this value is determined by dividing the photocurrent measured at the photoionization energy by the quantum yield of photoelectrons from the gold-plated copper plate at that photoionization energy[23]), and σ_{Cl/Cl^+} is the photoionization cross section of Cl at 13.68 eV averaged over the synchrotron bandwidth. For these calculations, we used the portion of the C−Cl bond fission $P(E_T)$ producing stable vinoxy predicted from our branching calculations (shown by the dashed gray line in Figure 3) and the photoionization cross section of Cl reported by Ruscic and Berkowitz[13] correcting for the lower cross section in the continuum beyond the ^1S_o threshold recommended by Berkowitz[14] based on subsequent studies. Because the TOF data for CH_3^+ were taken at two different ionization energies, we estimated the partial cross section at both ionization energies. The calculations for the partial cross sections are shown below.

$$\frac{1}{1} = \left(\frac{0.016845}{0.00100}\right) \times \left(\frac{1}{0.7578}\right) \times \left(\frac{16248}{12565}\right) \times \left(\frac{10.8\ \mu A/0.035}{26.1\ \mu A/0.106}\right) \times \left(\frac{\sigma_{CH_2CHO/CH_3^+}@10.5\ eV}{22.8\ Mb}\right) \quad (2)$$

$$\frac{1}{1} = \left(\frac{0.016845}{0.001585}\right) \times \left(\frac{1}{0.7578}\right) \times \left(\frac{16248}{12565}\right) \times \left(\frac{14.7\ \mu A/0.060}{26.1\ \mu A/0.106}\right) \times \left(\frac{\sigma_{CH_2CHO/CH_3^+}@11.44\ eV}{22.8\ Mb}\right) \quad (3)$$

We found the partial photoionization cross section of vinoxy appearing at CH_3^+ to be 0.63 and 1.3 Mb at ionization energies of 10.5 and 11.44 eV, respectively. It is important to note that when accumulating the signal at m/z = 15 at 11.44 eV, we alternated scans with m/z = 35 to average out any drifts in beam intensity or laser power; however, the signal at 10.5 eV was not taken with this precaution; therefore, the partial cross section at this photoionization energy should be regarded as preliminary.

Figure 4 shows the TOF spectrum taken at m/z = 29 (HCO^+) with a source angle of 20° and at an ionization energy of 11.53 eV. This spectrum also has a fast, sharp peak at ~35 μs that is consistent with dissociative ionization of stable vinoxy radicals in the ionizer; this contribution is fit by the dashed gray line and was derived from the portion of the C−Cl bond fission $P(E_T)$ producing stable vinoxy radicals (shown by the dashed gray line in Figure 2). By integrating the signal under this fit and comparing it to the momentum-matched contribution in the m/z = 35 TOF spectrum taken at the same source angle, we

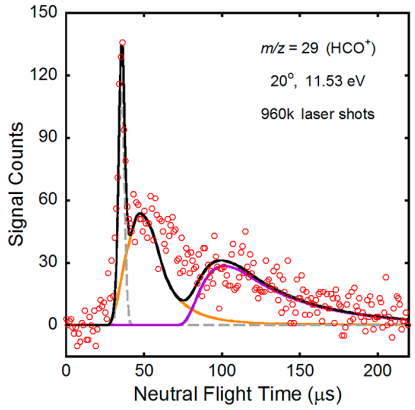

Figure 4. TOF spectrum taken at m/z = 29 (HCO^+) with a source angle of 20° and an ionization energy of 11.53 eV. Data are shown with red circles. The contribution from neutral HCO fragments formed by C−C bond fission in chloroacetaldehyde is fit by the solid orange line using the $P(E_T)$ shown in ref 22. The signal from the dissociative ionization of stable vinoxy to HCO^+ is shown by the fit with a dashed gray line calculated from the portion of the C−Cl bond fission $P(E_T)$ producing stable vinoxy radicals (shown with a dashed gray line in Figure 2). The fit shown with a solid purple line is the contribution attributed to photodissociation of clusters in the molecular beam. Because not all of the signal is accounted for by the fits, there is likely another source of m/z = 29.

DOI: 10.1021/acs.jpca.7b04730
J. Phys. Chem. A 2017, 121, 6262−6268

determined a partial photoionization cross section for vinoxy appearing at HCO^+, σ_{CH_2CHO/HCO^+}. However, we did not take the same precautions in taking alternating scans between m/z = 35 and 29, and we note that there is still signal left unfit (see ref 22 for further discussion). We therefore only report a rough estimate for the partial photoionization cross section and the ratio of this cross section to that of vinoxy to CH_3^+. The calculation of the partial cross section is given below.

$$\frac{\phi_{Cl}}{\phi_{CH_2CHO}} = \frac{1}{1} = \text{obs}\left(\frac{^{35}Cl^+}{HCO^+}\right) \times f_{^{35}Cl}{}^{-1} \times \text{TS}\left(\frac{CH_2CHO}{^{35}Cl}\right) \times \left(\frac{q_X}{q_{13.68\,eV}}\right) \times \left(\frac{\sigma_{CH_2CHO/HCO^+}}{\sigma_{Cl/Cl^+}@13.68\text{ eV}}\right) = \left(\frac{0.012071}{0.000546}\right) \times \left(\frac{1}{0.7578}\right) \times \left(\frac{4019}{3111}\right) \times \left(\frac{14.8\ \mu A/0.057}{26.1\ \mu A/0.106}\right) \times \left(\frac{\sigma_{CH_2CHO/CH_3^+}@11.53\text{ eV}}{22.8\text{ Mb}}\right) \quad (4)$$

We found the partial photoionization cross section to be 0.57 Mb at an ionization energy of 11.53 eV. This value differs from the partial photoionization cross section of vinoxy to CH_3^+ at 11.44 eV by a factor of 2. Thus, dissociative ionization to HCO^+ is also an important fate for photoionized vinoxy radicals.

To support the observation of dissociative ionization of vinoxy to CH_3^+ and HCO^+, we were also motivated to characterize critical points on the potential energy surface of the vinoxy cation shown in Figure 5. The stationary points and transition states along the cationic surface were calculated at the G4//B3LYP/6-311++G(3df,2p) level of theory and include zero-point energy corrections. We also provide the energies that are calculated using the available data from the Active Thermochemical Tables[24] for comparison to our G4 calculations. The calculated energies suggest that vinoxy with low internal energies could dissociatively ionize to CH_3^+ at photoionization energies near 10.4 eV; the dissociative ionization would be shifted lower in energy for vinoxy radicals with higher internal energy. We also note that there are two geometries located around the "vertical" ionization energy for vinoxy reported by Lee et al. and Savee et al. (10.3 eV):[10,11] rotTS$^+$, which represents a TS on the singlet cationic surface for rotation of the CH_2 moiety, and triplet vinoxy cation.

4. DISCUSSION

The data presented here provide the first estimates of the partial photoionization cross section of vinoxy to CH_3^+ at 10.5 and 11.44 eV as well as a rough estimate for the partial photoionization cross section of vinoxy to HCO^+ at 11.53 eV. Such values are of immense importance in the characterization of product branching and, more generally, in the study of gas-phase reaction dynamics. Because vinoxy radicals typically dissociate upon photoionization, these cross sections provide insight into the fate of vinoxy radicals following photoionization and the amount of signal from dissociative ionization of vinoxy expected at the daughter ion masses. Our estimates for the cross sections of vinoxy to CH_3^+ are consistent with the upper limit for the cross section value of 5.2 Mb determined from the data of Savee et al. in their study on the $O(^3P)$ + propene reaction.[11] That value is an upper limit due to potential contributions from the dissociative ionization of other larger

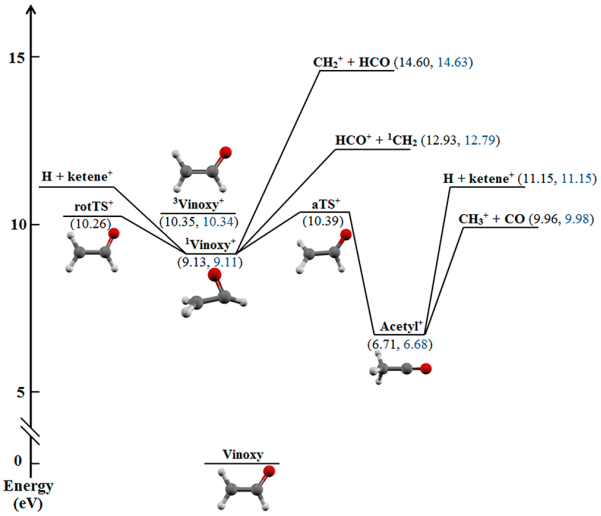

Figure 5. Selected minima and transition states on the cationic potential energy surface of vinoxy radical. The energies of the stationary points relative to the zero-point level of ground-state vinoxy are given in parentheses. The values in black were calculated at the G4//B3LYP/6-311++G(3df,2p) level of theory and include zero-point energy corrections; the values in blue are calculated from the available Active Thermochemical Tables data.[24] We note that the IUPAC name of the singlet vinoxy cation is oxiranilium. On the basis of the "vertical" ionization energy calculated by Lee et al. and Savee et al. (10.3 eV), it is likely that the excitation is either to rotTS$^+$ or the triplet vinoxy cation (which then must undergo internal conversion to the singlet cation to undergo dissociative ionization to m/z = 15 at the energies in this work).

species to CH_3^+. One of the benefits of using the chloroacetaldehyde system is that there are no larger species undergoing dissociative ionization as vinoxy is the only source of neutral CH_3 (from unimolecular dissociation/multiphoton dissociation) and CH_3^+. It was also easy to identify the signal from stable vinoxy in the m/z = 15 and 29 TOF spectra by momentum-matching with the high-kinetic-energy Cl photofragments. This identification could not be made in the previous velocity map imaging study because that apparatus characterizes the net velocity of the photoionized fragments, which is the vector sum of stable neutral vinoxy radicals and the recoil velocity imparted during the dissociative ionization of the neutral vinoxy radical to CH_3^+ or HCO^+. This recoil smears out the velocity distribution of the neutral fragment, making it hard to distinguish between CH_3^+ from dissociative ionization of neutral vinoxy radicals and CH_3 from the unimolecular dissociation of high-internal-energy neutral vinoxy radicals (see the Supporting Information).

It is worth noting that the error in these estimates is primarily dependent on the amount of signal in the TOF spectrum taken at m/z = 35 (Cl^+) that we attribute to primary C−Cl bond fission and the photoionization cross section of Cl. The scattering data show evidence of more high-kinetic-energy dissociation events (see the Supporting Information) than were previously observed in our velocity map imaging study.[17] Because we use the C−Cl bond fission $P(E_T)$ derived from the scattering data for all subsequent calculations, it is possible that we are overestimating the signal from C−Cl bond fission. If this is the case, our estimates of σ_{CH_2CHO/CH_3^+} would be too small. Compared to the previous velocity map imaging study, the

DOI: 10.1021/acs.jpca.7b04730
J. Phys. Chem. A 2017, 121, 6262−6268

NSRRC data show additional fast signal in the TOF data taken at m/z = 35 (Cl^+) that could be from a multiphoton process or dissociation of monomer or dimer hydrates of the precursor. While the assignment of the fast signal in the TOF data taken at m/z = 35 (Cl^+) would alter the C−Cl bond fission $P(E_T)$ and therefore the portion resulting in stable vinoxy, we get a comparable fit to the peaks from dissociative ionization in the TOF spectra taken at m/z = 15 (CH_3^+) using the stable portion of the C−Cl bond fission $P(E_T)$ derived in the velocity map imaging study. It is thus possible that the $P(E_T)$'s derived in the two studies differ because of calibration errors in the two instruments.[25,26]

While there have been no reported values for the partial photoionization cross section of vinoxy to CH_3^+, Lee et al. and Savee et al. report that the threshold for the dissociative ionization of vinoxy to CH_3^+ is 10.3 eV. Interestingly, the calculated barrier to forming CH_3^+ + CO is 10.4 eV relative to the zero-point level of the vinoxy radical; this is consistent with the appearance energy of CH_3^+ from vinoxy noted by Lee et al. and Savee et al.[10,11] However, the appearance energy depends on the internal energy of the vinoxy fragments, and thus, we may expect to see dissociative ionization at lower photoionization energies. By energy conservation, the average vibrational energy of the stable vinoxy radicals from C−Cl bond fission in this study is 33.5 kcal/mol. On the basis of this vibrational energy, we could in principle detect CH_3^+ from dissociative ionization of vinoxy at a much lower photoionization energy of 9.4 eV. While TOF data was also taken at m/z = 15 and a photoionization energy of 9.845 eV, the spectrum did not evidence significant signal from dissociative ionization of vinoxy radicals. We therefore cannot provide further evidence of the appearance energy threshold of CH_3^+ from vinoxy. While the predicted appearance energy threshold of HCO^+ from the G4 calculations is larger than the ionization energy used to take the m/z = 29 TOF spectrum, the average vibrational energy of the stable vinoxy radicals is enough to lower the appearance threshold. Therefore, the observation of HCO^+ from vinoxy at 11.53 eV is consistent with our computations.

The prior analysis assumes that the vinoxy radical is excited to its singlet cationic surface following photoionization. Excitation to the singlet cationic surface can occur via the transition state for rotation of the CH_2 moiety, rotTS$^+$, which has a calculated G4 energy close to the vertical ionization energy of vinoxy determined by Lee et al. and Savee et al.[10,11] and a very similar geometry to the ground-state vinoxy allowing for Franck−Condon overlap. For completeness, we also note the possibility of excitation to the triplet cationic surface via the triplet vinoxy cation. This stationary point also has a very similar geometry to ground-state vinoxy as well as a calculated G4 energy close to the vertical ionization energy of vinoxy. The G4 energy calculated for this stationary point is also consistent with the data provided in the Active Thermochemical Tables.[24] The triplet vinoxy cation, however, may not adiabatically dissociate to m/z = 15 at 10.5 eV; the triplet state correlates adiabatically to $^3CH_3^+$ and ^1CO products at an energy near 13.5 eV. Thus, the dissociative ionization of the vinoxy radical likely proceeds on the singlet surface with critical points shown in Figure 5.

■ ASSOCIATED CONTENT

Supporting Information

The Supporting Information is available free of charge on the ACS Publications website at DOI: 10.1021/acs.jpca.7b04730.

Comparison of the C−Cl bond fission $P(E_T)$'s derived from the velocity map imaging and scattering apparatuses and $P(v_{net})$ for m/z = 15 (CH_3^+) derived from the velocity map imaging apparatus (PDF)

■ AUTHOR INFORMATION

ORCID

Laurie J. Butler: 0000-0001-6965-3438

Notes

The authors declare no competing financial interest.

■ ACKNOWLEDGMENTS

This work was supported by the Chemical Sciences, Geosciences and Biosciences Division, Office of Basic Energy Sciences, Office of Science, U.S. Department of Energy, under Grant DE-FG02-92ER14305 (L.J.B.). Synchrotron beam time and additional funding were provided by the National Synchrotron Radiation Research Center and Academia Sinica. We gratefully thank Mr. Wen-Jian Huang and Dr. Yi-Lun Sun for their assistance in maintaining and using the apparatus at the NSRRC. We also thank Dr. Matthew D. Brynteson for his assistance with data collection.

■ REFERENCES

(1) Blank, D. A.; Suits, A. G.; Lee, Y. T.; North, S. W.; Hall, G. E. Photodissociation of Acrylonitrile at 193 nm: A Photofragment Translational Spectroscopy Study Using Synchrotron Radiation for Product Photoionization. *J. Chem. Phys.* **1998**, *108*, 5784−5794.

(2) Blank, D. A.; Sun, W.; Suits, A. G.; Lee, Y. T.; North, S. W.; Hall, G. E. Primary and Secondary Processes in the 193 nm Photodissociation of Vinyl Chloride. *J. Chem. Phys.* **1998**, *108*, 5414−5425.

(3) Blank, D. A.; North, S. W.; Stranges, D.; Suits, A. G.; Lee, Y. T. Unraveling the Dissociation of Dimethyl Sulfoxide Following Absorption at 193 nm. *J. Chem. Phys.* **1997**, *106*, 539−550.

(4) Cool, T. A.; Wang, J.; Nakajima, K.; Taatjes, C. A.; Mcllroy, A. Photoionization Cross Sections of Reaction Intermediate in Hydrocarbon Combustion. *Int. J. Mass Spectrom.* **2005**, *247*, 18 and references within..

(5) Balucani, N.; Leonori, F.; Casavecchia, P.; Fu, B.; Bowman, J. M. Crossed Molecular Beams and Quasiclassical Trajectory Surface Hopping Studies of the Multichannel Nonadiabatic $O(^3P)$ + Ethylene Reaction at High Collision Energy. *J. Phys. Chem. A* **2015**, *119*, 12498−12511.

(6) Leonori, F.; Balucani, N.; Nevrly, V.; Bergeat, A.; Falcinelli, S.; Vanuzzo, G.; Casavecchia, P.; Cavallotti, C. Experimental and Theoretical Studies on the Dynamics of the $O(^3P)$ + Propene Reaction: Primary Products, Branching Ratios, and Role of Intersystem Crossing. *J. Phys. Chem. C* **2015**, *119*, 14632−14652.

(7) McKee, K. W.; Blitz, M. A.; Cleary, P. A.; Glowacki, D. R.; Pilling, M. J.; Seakins, P. W.; Wang, L. Experimental and Master Equation Study of the Kinetics of OH + C_2H_2: Temperature Dependence of the Limiting High Pressure and Pressure Dependent Rate Coefficients. *J. Phys. Chem. A* **2007**, *111*, 4043−4055.

(8) Westbrook, C. K.; Dryer, F. L. Chemical Kinetics and Modeling of Combustion Processes. *Symp. Combust., [Proc.]* **1981**, *18*, 749−767.

(9) Brezinsky, K. The High-Temperature Oxidation of Aromatic Hydrocarbons. *Prog. Energy Combust. Sci.* **1986**, *12*, 1−24.

(10) Lee, S.-H.; Huang, W.-J.; Chen, W.-K. Dynamics of the Reaction of Atomic Oxygen with Ethene: Observation of All Carbon-Containing Products by Single-Photon Ionization. *Chem. Phys. Lett.* **2007**, *446*, 276−280.

DOI: 10.1021/acs.jpca.7b04730
J. Phys. Chem. A 2017, 121, 6262−6268

(11) Savee, J. D.; Welz, O.; Taatjes, C. A.; Osborn, D. L. New Mechanistic Insights to the $O(^3P)$ + Propene Reaction from Multiplexed Photoionization Mass Spectrometry. *Phys. Chem. Chem. Phys.* **2012**, *14*, 10410−10423.
(12) Scrape, P. G.; Roberts, T. D.; Lee, S.-H.; Butler, L. J. Dissociation Pathways of the CH_2CH_2ONO Radical: NO_2 + Ethene, NO + Oxirane, and a Non-Intrinsic Reaction Coordinate HNO + Vinoxy Pathway. *J. Phys. Chem. A* **2016**, *120*, 4973−4987.
(13) Ruscic, R.; Berkowitz, J. Photoionization of Atomic Chlorine. *Phys. Rev. Lett.* **1983**, *50*, 675−678.
(14) Berkowitz, J. *Atomic and Molecular Photoabsorption: Absolute Total Cross Sections*; Academic: San Diego, CA, 2002.
(15) Lau, K.-C.; Liu, Y.; Butler, L. J. Photodissociation of 1-Bromo-2-butene, 4-Bromo-1-butene and Cyclopropylmethyl Bromide at 234 nm Studied Using Velocity Map Imaging. *J. Chem. Phys.* **2006**, *125*, 144312.
(16) Krisch, M. J.; Miller, J. L.; Butler, L. J.; Su, H.; Bersohn, R.; Shu, J. Photodissociation Dynamics of Ethyl Ethynyl Ether: A New Ketenyl Radical Precursor. *J. Chem. Phys.* **2003**, *119*, 176−186.
(17) Lam, C.-S.; Adams, J. D.; Butler, L. J. The Onset of H + Ketene Products from Vinoxy Radicals Prepared by Photodissociation of Chloroacetaldehyde at 157 nm. *J. Phys. Chem. A* **2016**, *120*, 2521−2536.
(18) Ratliff, B. J.; Alligood, B. W.; Butler, L. J.; Lee, S.-H.; Lin, J. J. Product Branching from the CH_2CH_2OH Radical Intermediate of the OH + Ethene Reaction. *J. Phys. Chem. A* **2011**, *115*, 9097−9110.
(19) Lin, J. J.; Chen, Y.; Lee, Y. Y.; Lee, Y. T.; Yang, X. Photodissociation Dynamics of CH_3Cl at 157.6 nm: Evidence for CH_2 (X^3B_1/a^1A_1) + HCl Product Channels. *Chem. Phys. Lett.* **2002**, *361*, 374−382.
(20) Lee, Y. T.; McDonald, J. D.; LeBreton, P. R.; Herschbach, D. R. Molecular Beam Reactive Scattering Apparatus with Electron Bombardment Detector. *Rev. Sci. Instrum.* **1969**, *40*, 1402−8.
(21) Zhao, X. CMLAB2, version 6/93, modified by J. D. Myers. This is an interactive version built on the original cmlab2 program. Ph.D. Dissertation, University of California, 1988.
(22) Adams, J. D. Product Branching in the Photodissociation of Chloroacetaldehyde and the Incorporation of Angular Momentum in Statistical Predictions of Product Branching. Ph.D. Dissertation, The University of Chicago, Chicago, IL, 2017.
(23) Samson, J. A. R. *Techniques of Vacuum Ultraviolet Spectroscopy*; John Wiley & Sons, Inc.: New York, 1967; pp 230−231.
(24) *Active Thermochemical Tables*. http://atct.anl.gov (accessed July 6, 2017).
(25) Ratliff, B. J.; Tang, X.; Butler, L. J.; Szpunar, D. E.; Lau, K.-C. Determining the $CH_3SO_2 \rightarrow CH_3 + SO_2$ Barrier from Methylsulfonyl Chloride Photodissociation at 193 nm Using Velocity Map Imaging. *J. Chem. Phys.* **2009**, *131*, 044304.
(26) Alligood, B. W.; FitzPatrick, B. L.; Glassman, E. J.; Butler, L. J.; Lau, K.-C. Dissociation Dynamics of the Methylsulfonyl Radical and Its Photolytic Precursor CH_3SO_2Cl. *J. Chem. Phys.* **2009**, *131*, 044305.

DOI: 10.1021/acs.jpca.7b04730
J. Phys. Chem. A 2017, 121, 6262−6268